Geosciences Journal
Vol. 10, No. 4, p. 369 − 389, December 2006

Sequence stratigraphy of Pyeongan Supergroup (Carboniferous-Permian), Taebaek area, mideast Korea

Hyun Suk Lee* *School of Earth and Environmental Sciences, Seoul National University, Seoul 151-747, Korea*
Petroleum and Marine Resources Division, Korea Institute of Geoscience and Mineral Resources, Daejeon 305-350, Korea
Sung Kwun Chough *School of Earth and Environmental Sciences, Seoul National University, Seoul 151-747, Korea*

ABSTRACT: This study focuses on the sequence stratigraphy of the Pyeongan Supergroup (Carboniferous-Permian), central-eastern Korea. The supergroup consists of about 1700-m-thick siliciclastic deposits, disconformably overlying the Joseon Supergroup (Cambro-Ordovician). The entire succession is represented by thirteen sedimentary facies which can be organized into seven facies associations (FAs) and, in turn, three sequence units. Sequence 1 constitutes FAs 1, 2, 3, and 4. FA 1 consists of conglomerate, sandstone and shale facies, and is bounded by a sequence boundary (SB 1) at the base. The overlying purple siltstone with interbedded massive sandstone and carbonate grainstone (FA 2) formed on a coastal plain during sea-level rise, which is transitional upward into black shale and patchy bioturbated carbonate packstone (FA 3) of lagoonal environments. The transition from FA 1 to 3 represents relative sea-level rise with small-scale fluctuations, i.e., transgressive systems tract. FA 4 consists of cross-stratified conglomerate and massive sandstone with black shale which prograded over lagoonal area, forming highstand systems tract (HST). Sequence 2 consists of FAs 5 and 6. Sequence boundary (SB 2) occurs at the transition between FAs 4 and 5. FA 5 is characterized by cross-stratified coarse sandstone and purple fine sandstone to siltstone of fluvial plain environments. It represents rapid change in depositional environments from shoreface to fluvial system. FA 6 comprises upward-fining units (massive sandstone to dark gray siltstone), suggestive of restricted bay environments during relative sea-level rise. Due to an abrupt fall in sea level, the basin was closed with thick fluvial deposits (FA7). Sequence 3 comprises planar and trough cross-stratified coarse sandstone and partly bioturbated purple fine sandstone to mudstone (FA 7). The entire succession represents deposition of a second order cycle of sea-level rise and fall during the period between the Carboniferous and the Permian. A reconstructed relative sea-level curve is concordant with eustasy in the Carboniferous, but discordant in the Permian, implying that the influence of local tectonic movements was dominant in the Permian.

Key words: Carboniferous, Permian, Pyeongan Supergroup, depositional environments, sea-level changes, sequence stratigraphy

1. INTRODUCTION

In the late Paleozoic era, the supercontinent Pangea formed by amalgamation of several continental masses (e.g., Yin and Nie, 1996; Scotese et al., 1999; Veevers, 2004). Six transgressive and regressive second-order eustatic cycles have been identified during this time (e.g., Ross and Ross, 1985, 1988; Golonka and Ford, 2000). These changes were recorded in sediment-fill architecture of basins along the coastline of the Paleotethys such as those in North China, South China and Mongolia (Chen et al., 1997; Liu et al., 1997; Traynor and Sladen, 1995; Izart et al., 2003). The Permo-Carboniferous intracratonic basin in the Sino-Korean Block was filled mainly with siliciclastic sediments in marginal marine to fluvial environments under allogenic controls.

The Sino-Korean Block was located in the east of the Paleotethys, drifting away from the Gondwana during the Carboniferous. The block progressively collided with the Mongolian plate and the South China Block in the Permian (Yin and Nie, 1996; Golonka and Ford, 2000). A tectonic reconstruction of the Sino-Korean Block in the Korean peninsula suggests that the Taebaeksan Basin was in close proximity to the Pyeongnam Basin, North Korea in the Permo-Carboniferous (Chough et al., 2000; Fig. 1). The successions in the Taebaeksan Basin are similar to those scattered across the Sino-Korean Block (Fig. 1A), where the disconformity with the underlying Cambro-Ordovician sequence is prevalent over the entire platform (Kim et al., 2000). The Taebaeksan Basin was located on the eastern margin of the Sino-Korean Block where an epeiric marine basin formed by westward transgression (Liu, 1990).

The upper Paleozoic coal-bearing siliciclastic strata (Pyeongan Supergroup) occur in the central-eastern Korean peninsula, formed in marginal marine to fluvial environments (Cheong, 1969; Kim, 1978; Ryu et al., 1997). The lower part of the Pyeongan Supergroup is dominated by quartzose sandstone, whereas the upper part contains abundant feldspars, implying a change in provenance (Lee, 1990a, 1990b; Yu et al., 1997; Ko et al., 1999). Detailed measurements of lithologic units and sedimentary facies from available sections of the Pyeongan Supergroup (Hwangji Group in Taebaek area, southern part of the Baegunsan syncline) have led to modifications of the lithostratigraphy (Lee and Chough, 2006; Table 1). In this paper, we focus on the sequence stratigraphy of the Permo-Carboniferous succes-

*Corresponding author: hyun0922@Kigam.re.kr

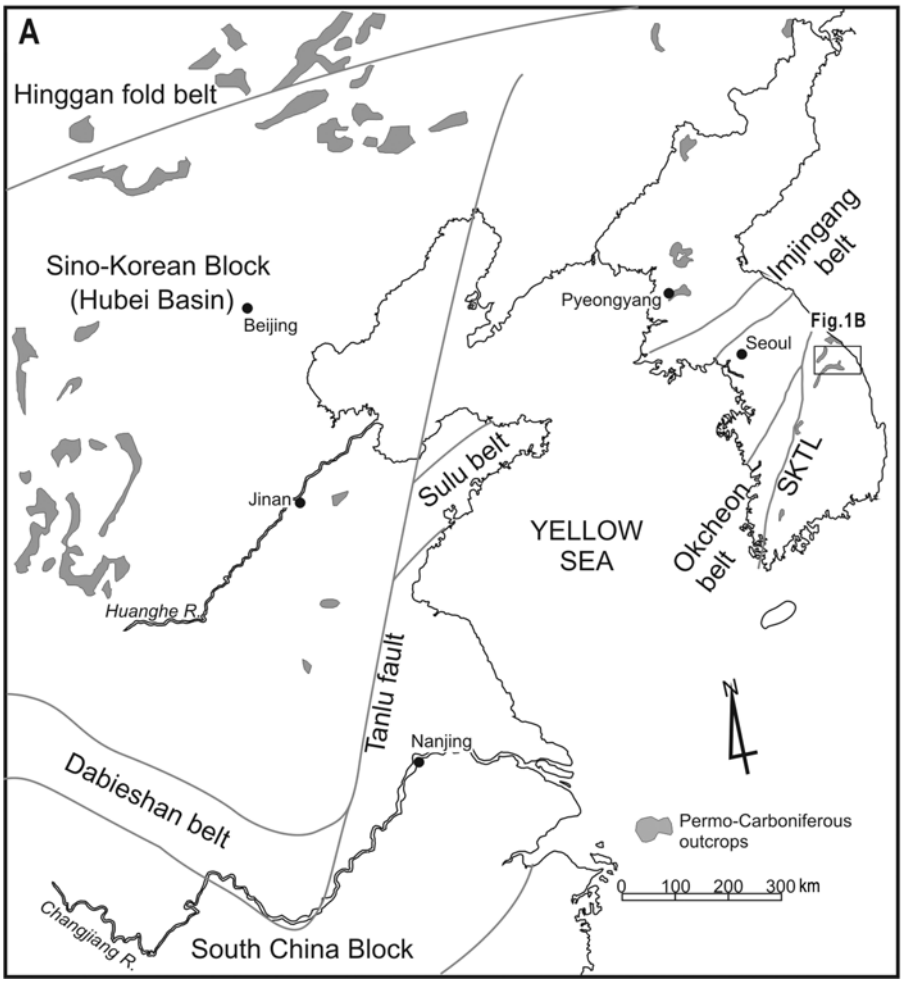

Fig. 1. **A**: Distribution of Carboniferous-Permian deposits in Sino-Korean Block and Korea. SKTL = South Korean Tectonic Line.

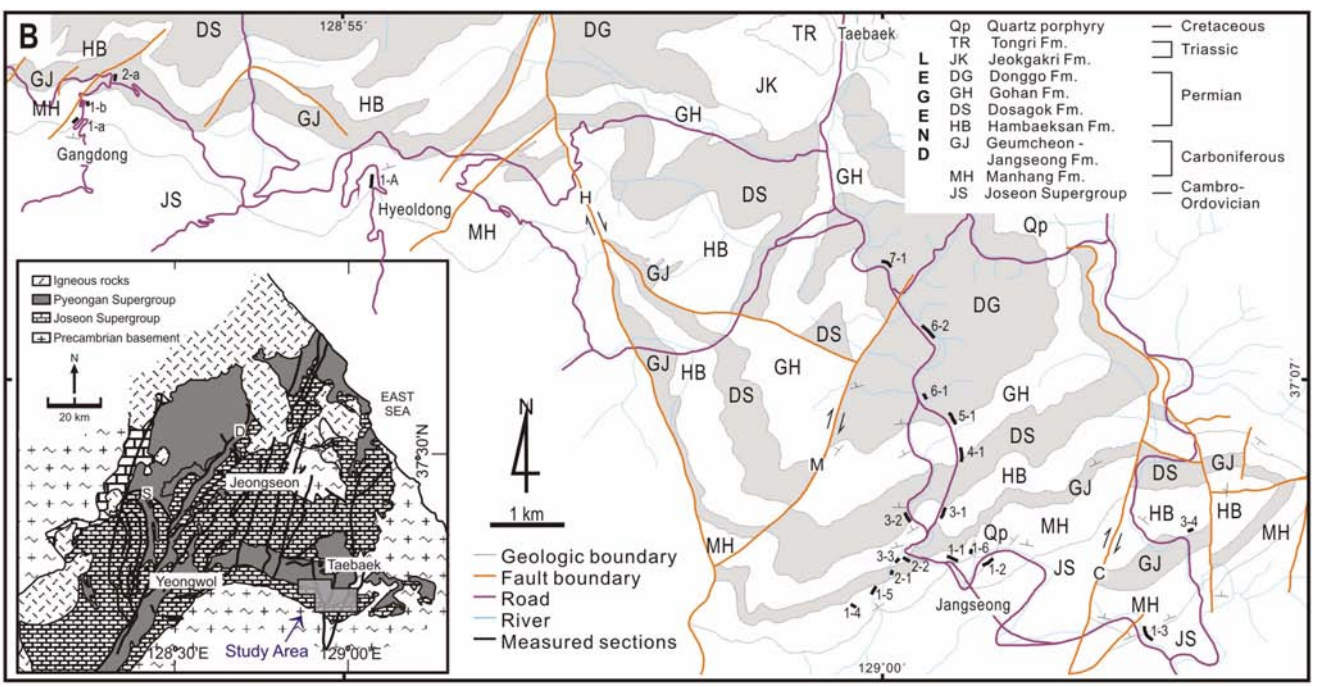

Fig. 1. (continued) **B**: Geologic map of the study area (modified from KIGAM, 1979). H = Hambaeksan fault, M = Mungok fault, C = Cheolam fault. Inset: D = Deokpori thrust fault, S = Seonwol thrust fault.

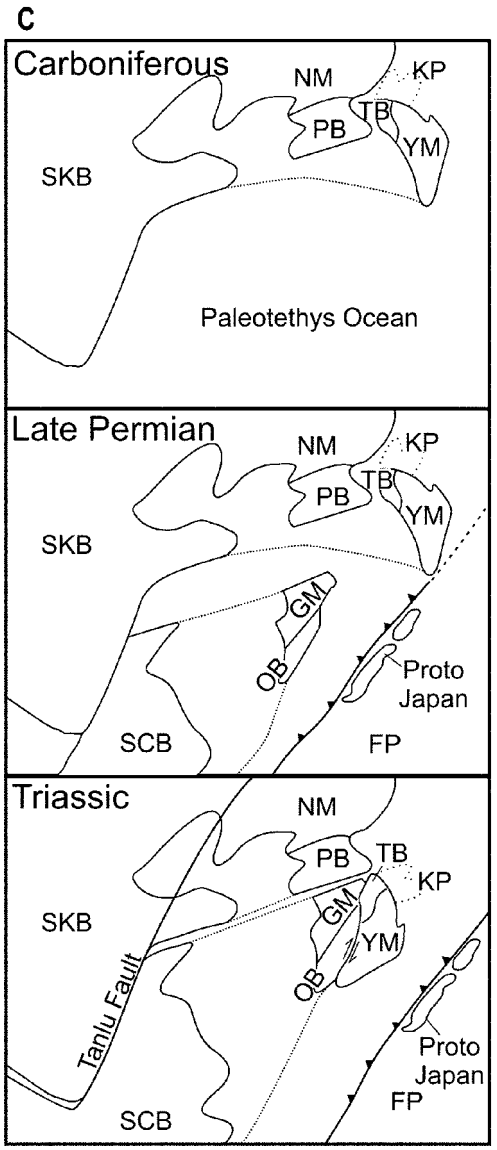

Fig. 1. (continued) **C**: Tectonic reconstruction of the Carboniferous, Late Permian and Triassic. SKB = Sino-Korean Block, SCB = South China Block, NM = Nangrim Massif, GM = Gyeonggi Massif, YM = Yeongnam Massif, PB = Pyeongnam Basin, TB = Taebaeksan Basin, OB = Okcheon Basin, KP = Korea Plateau, FP = Farallon Plate.

sion in the Taebaeksan Basin and further its implications in the eastern margin of the Sino-Korean Block.

2. GEOLOGIC SETTING

The Pyeongan Supergroup (Carboniferous-Permian) in the central-eastern part of the Korean peninsula is a thick siliciclastic succession (conglomerate, sandstone, and siltstone), which disconformably overlies the Joseon Supergroup (Cambro-Ordovician). The succession forms part of the Permo-Carboniferous succession in the Sino-Korean Block (Fig. 1A). The Pyeongan Supergroup was initially designated in the Taebaek area by Japanese workers and GICTR (1962) as Hongjeom, Sadong, Gobangsan and Nogam series (formations), following the scheme of the Pyeongan System in the Pyeongnam Basin of North Korea. Cheong (1969) established a stratigraphic scheme in the Taebaek area and divided the Pyeongan Supergroup into three groups and seven formations (Table 1). However, these units were lithologically poorly defined due to the lack of detailed measured sections. Cheong (1969) placed the group boundaries at perceived geochronological boundaries, without reference to the lithological changes. Lee and Chough (2006) have recently refined the lithostratigraphy of the succession based on detailed mapping of all available sections in the Taebaek area. The Hwangji Group comprises the Manhang, Geumcheon-Jangseong, Hambaeksan, Dosagok, Gohan and Donggo formations in ascending order (Table 1).

Cheong (1973) recognized three fusulinid zones in the Manhang Formation: *Eostaffella subsolana* Zone, *Beedeina mayiensis* Subzone and *Pseudostaffella kimi* Subzone of the early to middle Moscovian age. Lee (1992) described some conodont fossils and established the *Idiognathoides sulcatus* zones of the lower to middle Morrowan and *Neognathodus bothrops* zone of the upper Atokan to the lower Desmoinesian. In the lower part of the Geumcheon-Jangseong Formation, Cheong (1973) reported marine fossils of the Moscovian age in patchy limestone layers. According to Chun (1985, 1987), the upper part of the formation includes abundant plant fossils such as *Annularia, Baiera, Tingia, Radicites* and *Strobilites*, which are indicative of the Early Permian (?Artinskian). In the overlying Hambaeksan Formation, plant fossils (*Annularia mucronata, Lobatannularia sinensis, Calamites suckowi, Sphenophyllum thonii, Pecopteris arborescence, Taeniopteris latecostata, Nemejecopteris feminaeformis* and *Plagiozamites oblongifolius*) are indicative of the Early Permian (?Kungurian) (Chun 1985, 1987). The Dosagok Formation includes plant fossils of the Permian age, such as *Lobatannularia, Sphenophyllum, Tingia, Glossozamites* and *Gigantopteris* (Shiraki 1940). The Gohan Formation also contains the Permian plant fossils: *Chiropteris, Desmopteris, Elatocladus, Pecopteris, Tingia, Lobatannularia heianensis, Taeniopteris mutinervis* and *Cordaites principalis* (Shiraki, 1940; Chun, 1985, 1987).

The lower part of the Pyeongan Supergroup represents the Upper Carboniferous, based on fusulinids (Cheong, 1969, 1973). Due to the lack of fossils, the geologic age of the upper part of the Pyeongan Supergroup was poorly defined, although plant fossils are indicative of the Late Permian. The upper boundary of the Pyeongan Supergroup with the overlying the Jeokgakri Formation is characterized by an angular unconformity (Fig. 1B). The Jeokgakri Formation formed in a piggy-back basin (e.g., Chough et al., 2000). Rhyolite bodies that were intruded into the Pyeon-

Table 1. Stratigraphic summary of the Pyeongan Supergroup. Dashed line represents unknown age.

Basin	Geologic Age / Workers	Carboniferous			Permian				Triassic		
Pyeongnam Basin	Kodaira (1924)	Pyeongan System									
	Kawasaki (1927)	Pyeongan System									
		Hongjeom Fm.	Sadong Fm.			Gobangsan Ser.			Nogsaegam Fm.		
	Tateiwa (1931)	Pyeongan System									
		Hongjeom Ser.	Sadong Ser.			Gobangsan Ser.			Nogam Ser.		
Taebaeksan Basin	Shiraki (1930)	Pyeongan System									
		Hongjeom Ser.	Sadong Ser.			Gobangsan Ser.			Nogam Ser.		
	GICTR (1962)	Hongjeom Ser.			Sadong Ser.				Gobangsan Ser.		Nogam Ser.
	Cheong (1969, 1973)	Pyeongan Supergroup									
		Gomog Group			Cheolam Group				Hwangji Group		
		Manhang Fm.	Geumcheon Fm.		Jangseong Fm.	Hambaeksan Fm.			Dosagok Fm.	Gohan Fm.	Donggo Fm.
	KIGAM (1979)	Pyeongan Supergroup									
		Manhang Fm.	Geumcheon Fm.		Jangseong Fm.	Hambaeksan Fm.	Dosagok Fm.	Gohan Fm.	Donggo Fm.		
	Lee and Chough (2006)	Pyeongan Supergroup									
		Hwangji Group									
		Manhang Fm.	Geumcheon-Jangseong Fm.			Hambaeksan Fm.	Dosagok Fm.	Gohan Fm.	Donggo Fm.		

Table 2. Description and interpretation of sedimentary facies.

Facies Code	Description	Interpretation
Crudely cross-stratified conglomerate (Ccd)	This facies is represented by either crudely cross-stratified conglomerate or disorganized clasts in moderately sorted sand to silt matrix. Clasts are well to moderately sorted and granule- to pebble- grade (max. dL=3 cm). Poorly sorted clasts are scarcely present. The clasts are subrounded to rounded and include dark gray mudstone chips. The matrix is partly abundant (more than 25 %). The crude stratifications are represented by discontinuous pebble-concentrated layers or gravel-grade trains and clusters with general parallel orientation of grains. Each facies unit ranges in thickness from 50 to 300 cm, but amalgamated beds reach up to 460 cm. Most units are generally tabular and laterally continuous in outcrop scale, whereas some are lenticular or wedged with a slight change in thickness. The lower bed boundary is commonly sharp and planar, although some beds are bounded by undulatory or erosional boundary. The upper boundary is either gradational or sharp.	Deposition by *en masse* of mixed sand and gravel with diffuse sheets by high-magnitude heavy-laden flows (Miall, 1977; Todd, 1989; Todd and Went, 1991).
Planar cross-stratified sandstone (Sp)	This facies consists of planar cross-stratified medium to very coarse sandstone and pebbly sandstone. Cross stratification is represented by alternation of either coarser and finer strata or gravelly and sandy strata. Cross set is 10 cm to a few decimeters thick and commonly solitary set. Each bed ranges in thickness from 30 cm to a few meters.	2-D dunes, linguoid dunes, or bar with slipface (Harms et al, 1982; Miall, 1996).
Trough cross-stratified sandstone (St)	The facies is represented by trough cross-stratified medium to very coarse sandstone and pebbly sandstone. pebbles and/or mudstone intraclasts are recognized at the base of some units. Each set is 1 cm to a few meters thick and set thickness generally is proportional to grain size.	3-D sandy dunes and ripples; infills of scour hollow (Miall, 1977; Collinson and Tompson, 1989).
Crudely cross-stratified sandstone (Scs)	The facies consists of poorly to moderately-sorted and well-rounded to subrounded coarse sandstone to granule-grade conglomerate and is characterized by crude cross-stratification with discontinuous granule trains or streaks. Each set is decimeter to a few meters thick. It shows sharp erosional lower boundary and gradational upper boundary in some beds. Each facies unit ranges in thickness from 150 to 300 cm	Traction-dominant subaqueous and subaerial stream flow; migration of medium to large-scale bedforms (Miall, 1977, 1996; Bridge, 1993).
Horizontally stratified sandstone (Sh)	This facies consists of moderately to well sorted, horizontally stratified (laminated) fine to coarse sandstone, gray to dark gray in color. Stratifications consist of alternation of coarse sand and fine sand or discontinuous trains of well sorted granule and sand grains. Each facies unit ranges in thickness from 60 to 380 cm.	Migration of either low-amplitude bed forms or upper flow regime plane bed (Bridge, 1981, 1993; Allen, 1984).
Massive sandstone (Sm)	The massive sandstone is represented by massive medium to coarse sandstone occasionally with some granules or mudstone chips (max. dL=2 cm). Grains are relatively well sorted and well rounded to subrounded. Each facies unit ranges in thickness from 40 to 500 cm and slightly changes in bed thickness in outcrop scale. Occasionally some beds are wedged or lenticular. The upper and lower bed boundaries are commonly planar and sharp, and often undulatory or irregular.	Plane bed migration in upper flow regime; bed boundary amalgamated by rapid deposition; rapid deposition from high-concentrated flow (Jo and Chough, 2001).
Purple sandstone (Spu)	The facies consists of moderately sorted medium sandstone to siltstone, showing high variation in grain size. Some beds are horizontally-stratified. It shows purple, dark red and chocolate in color. Granule to coarse sand trains or streaks, calcite concretion and bourrows are commonly recognized.	Overbank or fluvial plain deposit (Miall, 1996).
Purple homogeneous mudstone (Fp)	The facies mainly consists of massive fine sandstone or homogeneous mudstone. Platy and blocky structures occur in some beds. In some cases, dark red mudstone chips occur in purple siltstone or fine sandstone and rimmed by gray contact. This facies varies in color from dark red, purple to purple mottled and mingled with gray. The gray parts are commonly coarser than the purple ones. In part, it is characterized by dispersed gray color and platy structures. Each facies unit ranges in thickness from 40 to 550 cm. The upper and lower boundaries are commonly sharp and planar or irregular.	Overbank deposits in coastal plain suggested by its fine grain size and slight bioturbation (Walker, 1967; Bentham et al., 1993).
Gray homogeneous mudstone (Fg)	The facies consists of massive fine sandstone and homogeneous mudstone. Occasionally, dark gray to black mudstone chips (max. dL=3 cm) or pyrites are dispersed. The mudstone chips are oriented parallel to bedding plane. In some cases, partly faint lamination occurs. The facies shows bright to dark gray, yellowish gray, greenish gray and milky white in color. The lower bed boundary is commonly gradational, whereas the upper is sharp. Each facies unit ranges in thickness from 10 to 350 cm.	Rapid sedimentation from suspended material; slightly bioturbated; post depostional graying under reducing condition (Miall, 1977; Turner, 1980).

Table 2. (continued)

Facies Code	Description	Interpretation
Laminated mudstone (Fl)	The facies is represented by parallel laminated siltstone (mudstone) and shale. The lamination is represented by an alternation of mudstone and siltstone. In part, the lamination is discontinuous and lenticular/wavy in centimeter-scale. Occasionally, finer laminae are commonly reddish. The lower laminae boundaries are erosional or sharp. Calcareous nodules or pyrites randomly occur. The lower and upper bed boundaries are generally sharp and planar. Each facies unit ranges in thickness from 40 to 400 cm.	Suspension settling affected by pulses of riverine inflows; deposition from bidirectional or periodic currents (Hjellbakk, 1997).
Black shale (Sb)	The Facies is represented by black shale or coaly shale. It contains abundant plant fossils such as *Annularia, Lobatannularia, Sphenophyllum,* and *Neuropteris*. Parallel discontinuous laminae are well or crudely developed in some part. Black shale beds are commonly squeezed and slipped into the upper or lower beds.	Marsh or swamp deposit; high nutrient supply and anoxic condition (McCabe, 1984; Cabrera and Saez, 1987).
Grainstone (Lg)	This facies is characterized by milky white to gray massive grainstone to packstone. The lime grains consist mainly of fossils such as brachiopods, foraminifera, and algae particles as well as siliciclastic clasts . This facies also contains quartz grains more than 5 %. In some cases, shale is intercalated with massive grainstone. The upper and lower boundaries are sharp and planar. These limestone units are a few decimeters to a few meters thick and commonly wedge-shaped or lenticular . This facies is commonly interlayered within puple silststone (Facies Fp) or gray siltstone (Facies Fg).	Storm sedimentation or deposition in coastal pond; deposits of intermediate subtidal zones, i.e., "flaser rocks"; fossil fragments are indicative of subtidal deposition (Allen, 1982; Aigner, 1985).
Bioturbated limestone (Lb)	This facies is represented by dark gray bioturbated packstone to wackestone with bioclastic fragments such as foraminifera and gastropod. Mottled texture is caused by selective dolomitization of burrows (ichnofacies index-2 or index-3). Horizontal or subhorizontal and subordinately vertical burrows are recognized. Each facies unit is more than 1 m in thickness. In some cases, wavy chert or shale is interlayered with bioturbated wackestone to packstone.	Intermediate or shallow subtidal deposits modified by bioturbation. The common presence of bioclastic fragments such as gastropod and foraminifera is suggestive of deposition in shallow subtidal with normal marine salinity (Roads, 1967; Heckel, 1972).

gan Supergroup and the Jeokgakri Formation are dated at 88.351±2.709 and 67.107±2.500 Ma, respectively. Chough et al. (2000) also suggested that sedimentation in the Taebaeksan Basin ceased prior to the major crustal deformation in the Triassic.

The entire succession was deformed in the Triassic when the Sino-Korean Block collided with the South China Block at the Imjingang belt (Ree et al., 1996) and drifted southwestward along the South Korean Tectonic Line (SKTL; Fig. 1A). In the southern part of the Baegunsan syncline the succession underwent a number of deformational events during this time (Kim and Won, 1987; Kim et al., 1988; Kim and Kee, 1991; Kim, 1994; Kim et al., 1994). The succession in the western part (Yeongwol area) is dominated by westward-dipping thrust faults, whereas the eastern part (Taebaek and Jeongseon areas) is dominated by oblique-slip faults and syncline with minor thrusts (Fig. 1B). Regional-scale thrust faults are prevalent between these areas, namely Deokpori and Gongsuwon thrust faults and others (Fig. 1B, inset). The Baegunsan syncline represents a large-scale N-S compressional deformation regime in which the entire Joseon and Pyeongan supergroups were folded and offset by NNE-SSW-running strike-slip faults, i.e., Hambaeksan and Cheolam faults (Fig. 1B).

3. SEDIMENTARY FACIES AND INTERPRETATION

Twenty-one well-exposed outcrop sections of the Pyeongan Supergroup were examined along road and stream cuts in the southeastern part of the Baegunsan syncline (Fig. 1B). Primary sedimentary structures and texture are preserved in most sections, although the strata were subject to strong deformation and weak to moderate metamorphism. The sedimentary facies and facies association are summarized, including sedimentary characteristics of grain size, mineralogy, sedimentary structures, bed geometry and fossil contents (Table 2, Figs. 2 and 3). Despite discontinuous exposure of succession and dimmed sedimentary structures by deformation, the sedimentary facies are organized into seven facies associations (Table 3).

4. SEQUENCE UNITS AND DEPOSITIONAL SYSTEMS

The disconformity (Fig. 4A) between the Duwibong (Joseon Supergroup) and Manhang formations represents a type-1 sequence boundary of Posamentier and Vail (1988) and Van Wagoner et al. (1988). Sequence 1 formed in shoreface environments with low-gradient prograding deltas off rivermouths (FA 1, Fig. 5A) during the initial transgressive phase. FA 1 is characterized by alternation of sheet- or

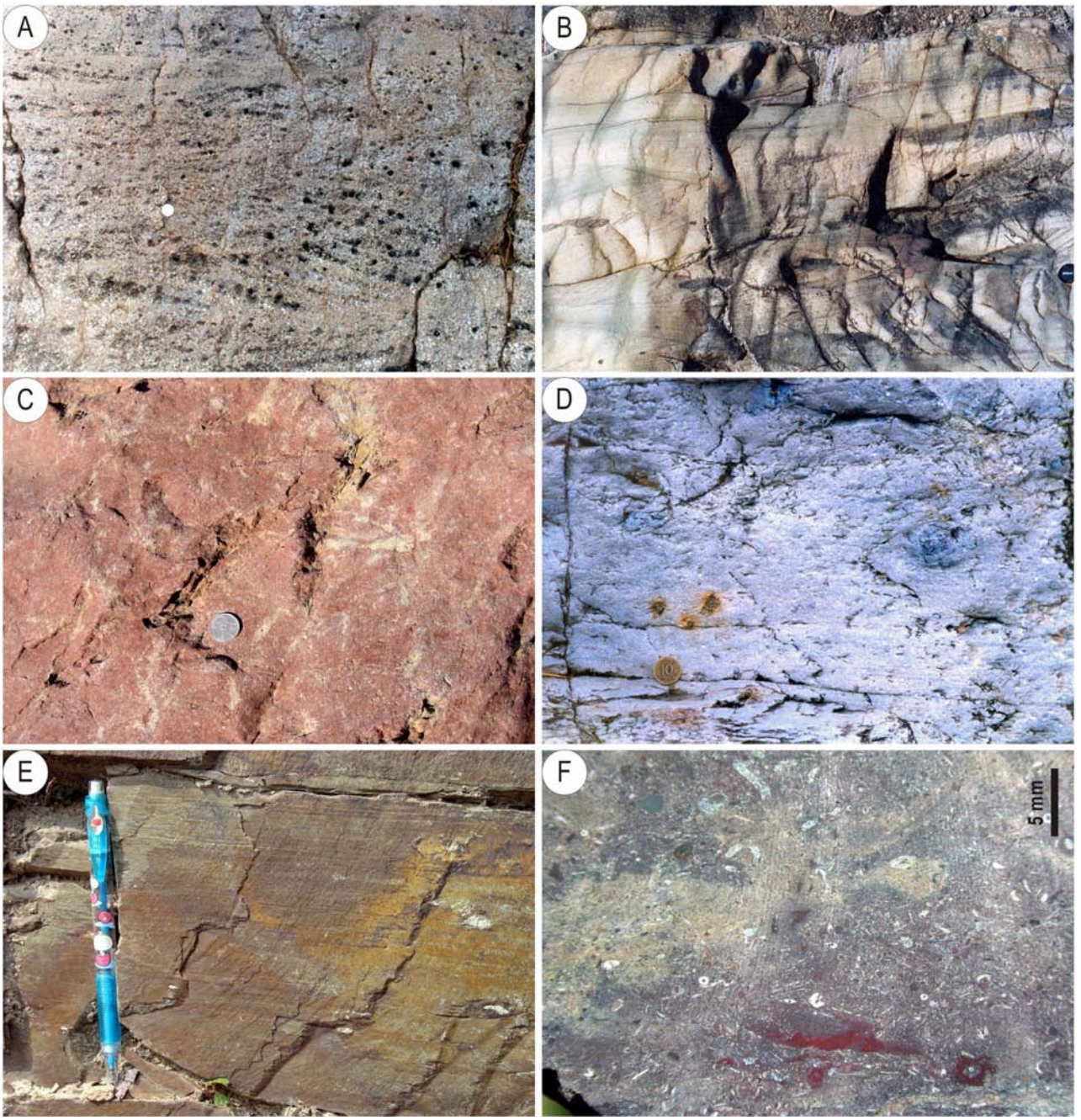

Fig. 2. Photographs of sedimentary facies in the Hwangji Group, Taebaek area. **A**: Crudely cross-stratified conglomerate, section 1-5 (FA 2), **B**: Planar and trough cross-stratified coarse sandstone (FA 7), **C**: Bioturbated purple or red sandstone, section 7-1 (FA 7), **D**: Gray homogeneous mudstone with pyrite and calcareous nodules, section 1-4 (FA 1), **E**: Gray parallel laminated mudstone, section 1-A (FA 1), **F**: Grainstone with purple mudchips, section 1-5 (FA 2). Coin for scale is 25 mm in diameter, lens cap 75 mm in diameter and pencil 142 mm long. For section location, see Figure 1B.

channel-shaped conglomerate and gray siltstone beds (Fig. 4B and C), and shows lateral variations in thickness and lithofacies, which indicates that sediments were supplied by local outlets of rivers. FA 1 is transitional to coastal plain environments with bedload-dominated braided system (FA 2). Cross-stratified conglomerate and bioturbated purple siltstone in FA 2 (Fig. 6A, B) were deposited in coastal plain and channels, whereas bioclastic grainstone beds formed in floodplain ponds frequently connected to open marine due to the fluctuation of water

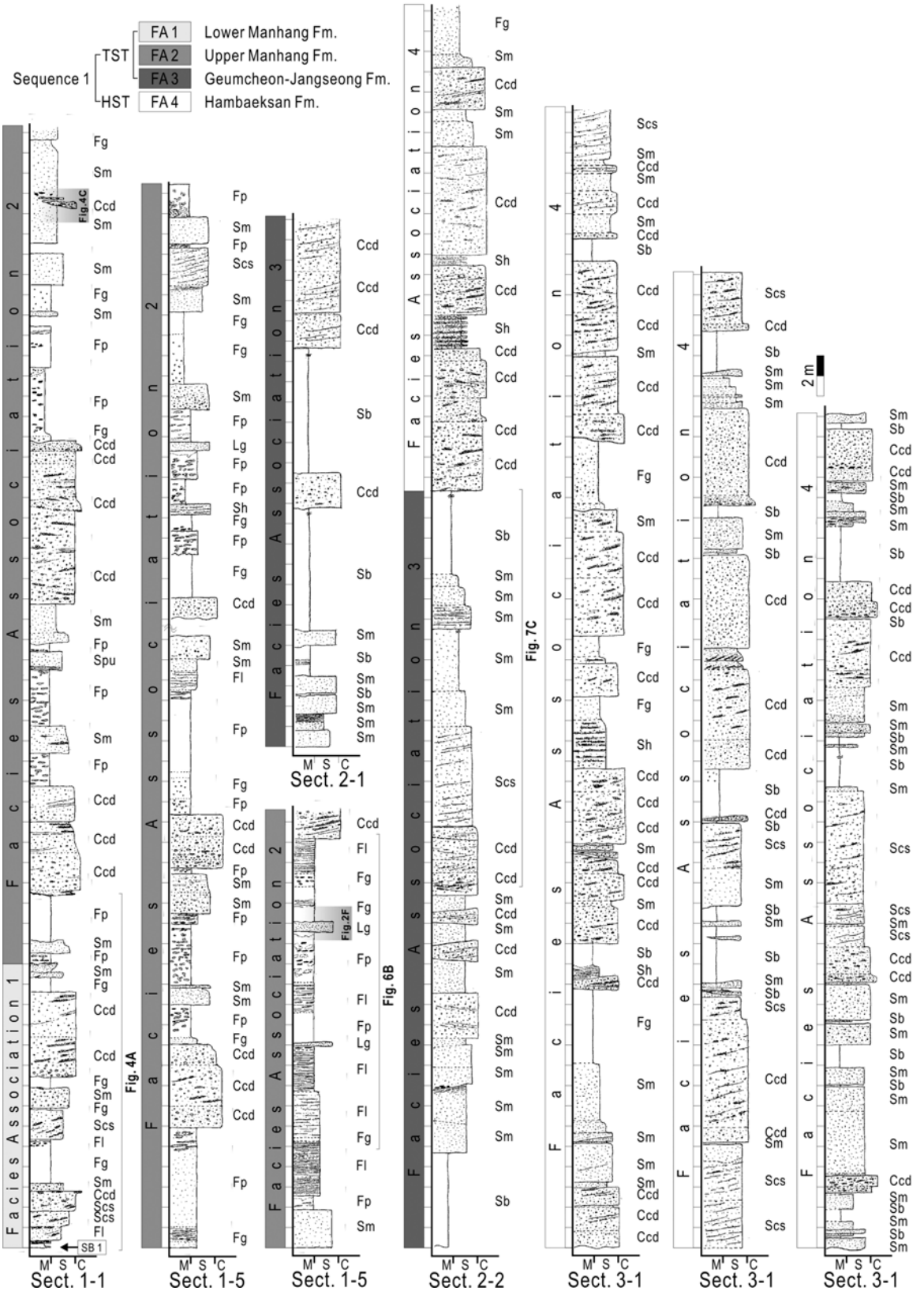

Fig. 3. Columnar descriptions of the Hwangji Group. Lithologic (formation) boundaries, facies association and sequence stratigraphic units are identified. Arrows indicate paleoflow directions based on measurements of cross-stratification. M = mudstone, S = sandstone, C = conglomerate. For abbreviation of sedimentary facies codes, see Table 2. For section location, see Figure 1B.

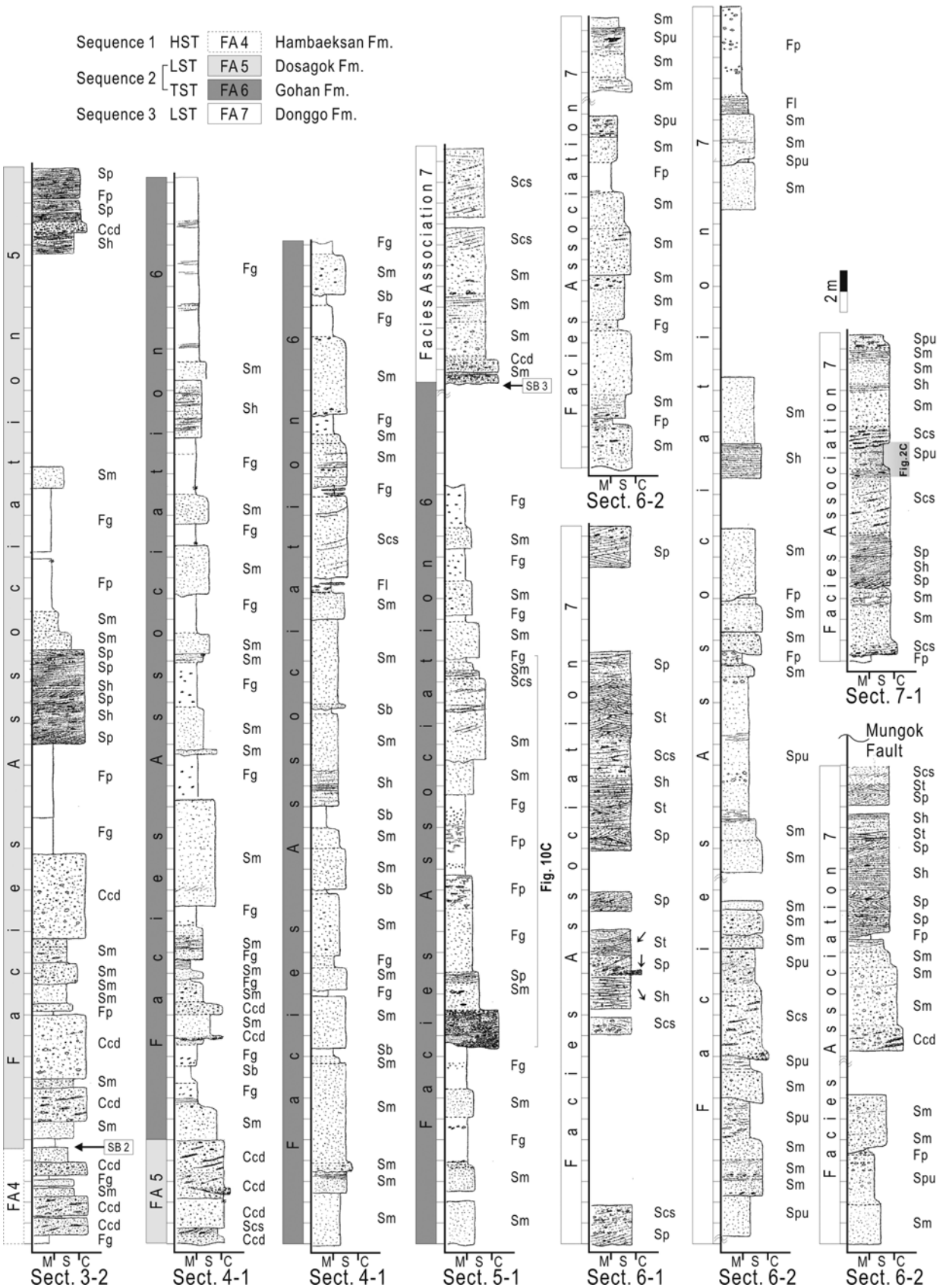

Fig. 3. (continued).

Table 3. Description and interpretation of facies associations (FA).

FA	Constituent	Description	Interpretation	Sections
1	Ccd, Sm, Fg (Scs, Fl, Sb)	Crudely cross-stratified conglomerate and coarse sandstone beds are stacked with sharp and undulatory lower boundaries and show sheet- or channel-shaped geometry. Gray siltstone beds are mostly homogeneous and vaguely laminated, and contain pyrite. Each bed is laterally continuous with slight thickness variations at outcrop scale. FA 1 thins eastward from 38 to 17 m, largely due to a decrease in conglomerate beds. In sections 1-a and 1-A, a disorganized conglomerate and massive sandstone bed formed the disconformity between the Joseon and the Pyeongan supergroups. It is overlain by slightly wavy-laminated dark gray mudstone and thick crudely cross-stratified or disorganized conglomerate with thickness variations. The base of section 2-1 is characterized by disorganized conglomerate and massive sandstone, which are overlain by thick homogeneous mudstone with mudchips. Elsewhere, laminated dark gray mudstone with limestone pebbles lies directly above the disconformity in section 1-1 (Fig. 4A). It grades vertically into crudely cross-stratified conglomerate, representing a ca. 4 meter thick coarsening-upward unit (Fig. 4B).	The upward-coarsening unit of gray massive conglomerate and sandstone beds indicates that sediments were supplied by local outlets of rivers, probably small-scale deltas with development of floodplains. Lateral changes in thickness and lithofacies reflect the variation of local sedimentary sources. The crudely cross-stratified, poorly sorted and well-rounded coarse-grained deposits most likely represent hyperconcentrated density flow in shoreface environments with abundant sediment supply (Todd, 1989). The interbedded dark gray homogeneous mudstone (Facies Fg) is suggestive of subaqueous conditions in interlobe or distal part of small deltas. Pyrite in the homogeneous mudstone formed in reducing conditions during or after deposition. This facies association represents shoreface environments with local sediment supply during the initial transgression.	1-1, 1-2, 1-3, 1-a, 1-A
2	Ccd, Sm, Fp (Lg)	Amalgamated and disorganized conglomerate beds are characterized by an erosional or sharp planar lower boundary and wedge-shaped geometry (Fig. 6A). Decimeter-scale channelized conglomerate and massive sandstone beds encased in homogeneous siltstone rarely occur in the middle part of the association (Fig. 4C). The thickness and number of conglomerate-dominated beds (Ccd and Sm) decrease upward, replaced by massive sandstone-dominated beds. The thickness of mudstone facies (Fp) increases upward (maximum of 8 m) (Fig. 3). Fining-upward units (from conglomerate or coarse sandstone to purple siltstone) are identified in the lower and middle parts of FA 2. A few discontinuous milky white to gray massive bioclastic pack-grainstone (Facies Lg) are interlayered with purple and gray siltstone in the upper part of FA 2 (Fig. 6B). They contain brachiopods, foraminifera and algae particles with siliciclastic clasts such as quartz and purple siltstone chips (Fig. 2F) and are a few decimeters to a few meters thick with sharp and planar boundaries.	Crudely-stratified conglomerate and massive sandstone probably represent deposits of hyperconcentrated density flow (Simpson et al., 2002). The lack of internal stratification and the poor sorting indicate en masse deposition. The en masse deposition of crudely cross-stratified conglomerate is succeeded by suspension settling of massive sandstone from waning flood flow. The intermingled or mottled purple and gray siltstones suggest that oxidizing conditions may have been unstable and changed into reducing conditions (Walker, 1967; Davies and Gibling, 2003). Massive bioclastic grainstone to packstone lenses formed in floodplain ponds that were frequently connected to open marine water during changes in sea-level and water table. Clastic sediments were transported in coastal floodplain environments by en masse deposition or accumulation on a variety of bars (Miall, 1978, 1985, 1996; Todd, 1989). Decrease of conglomerate beds, increase of purple mudstone facies, intercalation of limestone lenses and fossils in grainstone are collectively indicative of coastal floodplain environments.	1-2, 1-3, 1-4, 1-5, 1-6, 1-A, 1-b
3	Sm, Sb, Lb (Ccd)	Coarse-to-medium sandstone beds are wedged, lobe- or planar-shaped in cross-section. Several horizons of shale beds (Facies Fg) occur with abundant brachiopods, bivalves and crinoids. The lower part of the association consists of alternating units of gray coarse sandstone and black shale, whereas the upper part comprises dark gray massive or cross-stratified coarse sandstone, fine sandstone and black shale. The uppermost part is characterized by meter-scale fining-upward units from cross-stratified conglomerate to black shale (Fig. 7C). In section 2-A (Fig. 7A), several meter-thick dark gray bioturbated, bioclastic wackestone and packstone beds occur with foraminifera and fusulinids (Fig. 7D-F). In section 2-1 (Fig. 7B), two decimeter-thick bioturbated lime mudstone lenses are interbedded with dark gray shale above the boundary between FAs 2 and 3. Bioturbated limestone beds are recognized in the lower part and show a regional variation in thickness, thinning eastward from 24 to 3m. Crinoid stems with cirri and articulated brachiopods occur in section 2-1 (Fig. 7G).	The planar and trough cross-stratified coarse sandstone beds formed by migration of progradational lagoonal bars (Miall, 1978). Dark gray massive sandstone and cross-stratified coarse sandstone beds were deposited in shoreface or sand barrier during the progradation or retrograding of clastic wedges. Crinoid stems with cirri and articulated brachiopods are indicative of restricted environments like a lagoon. The lack of associated rootlet horizons or seat earth suggests that the coals were allochthonous (Cabrera and Saez, 1987). Bioturbated limestone is interpreted as an intermediate or shallow subtidal deposit out of lagoon. The abundant occurrence of horizontal and slightly inclined burrows is suggestive of shallow subtidal deposition (Rhoads, 1967). The common occurrence of biogenic grains such as disarticulated brachiopods, fusulinid and foraminifera in wedge-shaped limestone beds is also suggestive of deposition in subtidal environments with normal marine salinity (Heckel, 1972). This association suggests deposition in lagoonal and subtidal environments.	2-1, 2-2, 2-a

Table 3. (continued).

FA	Constituent	Description	Interpretation	Sections
4	Ccd, Sm, Sb (Scs)	Conglomerate and coarse sandstone beds are crudely cross-stratified, which are characterized by discontinuous pebble-concentrated layers and gravel trains and clusters with parallel orientation of grains. Most conglomerate beds are generally tabular in cross-section and laterally continuous at outcrop scale (Fig. 8A). In the lowermost part of the association, cross-bedded coarse sandstone prograded westward and southward direction (Fig. 8B). The laminated black shale beds are characterized by sharp and planar boundaries. Conglomerates beds are amalgamated. In the lower part of the association, coarsening-upward units comprise black shale or dark gray fine sandstone and cross-stratified or disorganized conglomerate. These units range in thickness from 8 to 20 m and thicken upward to the middle part of the section (Fig. 3).	The coarse-grained deposits in this facies association most likely represent high-concentration traction currents off river mouths during floods with abundant sediment supply (Todd, 1989). The polymodal grain-size distribution, locally abundant matrix, immature internal sedimentary structures, discontinuous gravel trains and crudely cross-stratified pebble alignments collectively suggest that sediments were deposited en masse with diffuse sheets by high-magnitude heavy-laden flows (Miall, 1977; Todd, 1989; Todd and Went, 1991; Nemec and Postma, 1993; Jo and Chough, 2001). The thickening-upward and prograding conglomerate units mostly represent the development of small-scale delta. The progradational lobe and sheet-shaped sandstones, and conglomerate beds were affected by localized sediment input and topography. The low-angle crude cross stratification is indicative of small-scale topographic irregularity. The interbedded gray homogeneous mudstone (Facies Fg) formed in the interlobe or proximal parts of small-scale deltas. This association represents deltaic progradation into lagoonal environments.	2-2, 3-1, 3-2
5	Scs, Sp, Sm, Fp (Ccd, Fg)	Massive sandstone and conglomerate beds are similar in lithology to those of FA 4, whereas coarse sandstone is characterized by well developed planar cross-stratification with tangential or angular basal contact and horizontal stratification (Facies Sp and Sh, Figs. 3 and 9). Cross- set thicknesses range from a few centimeters to decimeters, and sets are characterized by erosional upper and lower boundaries. The sandstone beds are moderately to well-sorted. Purple siltstone and fine sandstone are generally homogeneous or massive with randomly dispersed quartz granules. In the lower and upper parts of the association, crudely cross-stratified conglomerate is dominant and purple siltstones are interbedded with massive coarse sandstone showing sharp boundaries. In the middle part, fining upward units from cross-stratified coarse sandstone and massive sandstone to purple siltstone are evident.	Planar cross-stratified sandstone and conglomerate are indicative of deposition in fluvial systems by migration of sand bars within channels (Miall, 1996). Especially, the co-occurrence of cross-stratified coarse sandstone and crudely cross-stratified conglomerate is suggestive of en masse deposition and accumulation of various bars (Miall, 1985; Todd, 1989). The fining upward trend from cross-stratified sandstone to purple siltstone is also suggestive of fluvial systems (Miall, 1977, 1978). The various depositional processes are related to a reduction in stream gradient resulting from a change in bar morphology through time and an increase in transport distances. Purple sandstone is indicative of oxidizing conditions in a subaerial environment. This facies association most likely formed in braided rivers in fluvial plains.	3-2
6	Sm, Fg, Sb (Ccd, Scs, Fp)	Most of sandstone beds are massive but partly stratified. Black mudstone chips occur within massive sandstone beds in the middle part of the association. Wavy medium sandstone beds occur locally within gray siltstone in the middle part of the facies association. Siltstone beds are mostly homogeneous and gray, yellowish gray, olive gray and dark gray in color with black mudstone chips. Gray siltstone beds are characterized by gradational lower and undulatory upper boundaries. Gray siltstone and black shale beds are partly laminated. Black shale thickens in the middle part of the association, up to 8 m (Fig. 3). Dark gray mudstone is abundant in the lower part of the association, whereas sandstone is dominant in the middle to upper part (Fig. 10A, B). Intraformational conglomerate and bioturbated purple fine sandstone to siltstone occur in the lower part of section 5-1 (Fig. 10C).	Black shale and gray siltstone were deposited by the settling of suspended materials in anoxic to suboxic conditions, which partly prohibited biogenic activity (McCabe, 1984). Lenticular-bedded gray medium sandstone and laminated mudstone indicate tidal effect (Plint and Wadsworth, 2003). In the upper part of section 4-1, the sheet or wavy medium sand layers intercalated with black shale are also indicative of tidal influence. The fining-upward units with erosional lower boundary represent tidally influenced restricted bays (Reading and Collinson, 1996; Einsele, 2000). Clasts in the oligomictic conglomerate bed are composed of laminated and massive mudstone and represent an intraformational conglomerate. These oligomictic clasts and randomly dispersed mudstone-chips indicate collapse of a mud bank or erosion of the underlying mud beds. The fining-upward units, bioturbation, anoxic to suboxic condition and tidal influence imply that FA 6 formed most likely in restricted bays.	4-1, 5-1

Table 3. (continued).

FA	Constituent	Description	Interpretation	Sections
7	Sp, St, Sm, Spu (Scs, Fp)	FA 7 can be divided into two units. The first one is represented by cross-stratified coarse sandstone (Facies Sp, Sh and Scs). It occurs in section 6-1, the uppermost part of sections 6-2 and 7-1. The unit mainly consists of coarse sandstone, intercalated with bioturbated purple siltstone and sandstone. The coarse sandstone beds are planar and trough cross-stratified, and generally wedge-shaped in cross-section (Fig. 3). The second unit is dominated by purple sandstone (Facies Spu) and occurs in the lower part of section 6-2. It is characterized by an upward-fining trend, from massive coarse sandstone (Facies Sm) to purple fine sandstone. Each bed boundary is gradational, but the lower boundary of upward-fining units is erosional (Fig. 3). Purple siltstone and fine sandstone beds are bioturbated and include calcite concretions.	The fining-upward sequence, well developed cross-stratification, purple siltstone with calcrete and abrupt changes in unit thickness are all indicative of deposition in fluvial environments (Miall, 1977, 1978). The first unit most likely formed in perennial braided channels, whereas the second unit formed in overbank environments. Planar cross-stratified coarse sandstone beds indicate migration of two-dimensional dunes or linguoid bars whereas trough cross-stratified coarse sandstones formed by 3-D dune migration (Miall, 1977, 1978). A limited number of paleocurrent measurements, derived from planar and trough cross-stratification indicate southward flow directions. Crudely cross-stratified coarse sandstone beds formed by traction-dominant flows at times of high discharge when braided channels formed a single broad shallow channel, causing crevasse splays on the flood plain. Crevasse-splay massive sandstone and bioturbated purple siltstone to fine sandstone with calcite concretions and purple siltstone chips are also suggestive of deposition on the floodplain.	5-1, 6-1, 6-2, 7-1

table. The development of stable coastal plain suggests that the rate of sea-level rise slowed. With ensuing rise in sea level, the floodplain was changed into lagoonal environments (FA 3, Fig. 5B). Limestone lenses and coal beds of FA 3 (Fig. 7A) formed in intermediate or shallow subtidal environments. Planar and trough cross-stratified coarse sandstone beds (Fig. 7B and C) were deposited by migration of lagoonal bars, forming restricted environments such as lagoon and swamp. These units (FAs 1, 2 and 3) are assigned to a transgressive systems tract (TST; Fig. 3). They contain brachiopods, fusulinids and plant fossils of the Moscovian to Artinskian (Fig. 7D-F). Sediments were derived from the north and east (Kim, 1978). The maximum flooding surface can be placed on the boundary between the uppermost black shale bed of FA 3 and conglomerate of FA 4 (Fig. 3). The black shale bed of FA 3 is the top of fining-upward unit and deformed by fault. The south-to-westward prograding foresets (Fig. 8B) and the coarsening- and thickening-upward units (FA 4) represent small-scale delta progradation in shoreface environments during stillstand of sea level (Fig. 5C). The interlobe or proximal part of small-scale deltas was filled with gray to greenish gray mudstone. The deposits of high density sediment-laden flow were preponderant in shoreface. FA 4 represents highstand systems tract (HST) of sequence 1 and contains the early Permian plant fossils (Kungurian).

Although relative sea-level fall was not great enough to form extensive erosion at the sequence boundary (SB 2), it is represented by a sudden change in sedimentary facies from facies associations 4 to 5 (Figs. 3 and 9). FA 5 consists of cross-stratified sandstone to conglomerate and purple fine sandstone, which is interpreted as deposits of fluvial system (Fig. 5C). Various sedimentary structures in FA 5 are related to a reduction in stream gradient, resulting from a change in bar morphology. FA 5 represents sea-level fall where shoreface prograded with a development of fluvial system. This unit is assigned to the lowstand systems tract of sequence 2 (LST; Fig. 3). With ensuing rise in sea level, fluvial plain with braided rivers changed into a restricted bay environment (FA 6, Fig. 5D), which is characterized by a fining-upward unit from massive sandstone to gray siltstone or black shale (FA 6, Fig. 10A, B, C). It represents transgressive systems tract with small-scale fluctuation, indicated by intraformational conglomerate and purple laminated siltstone (TST; Fig. 3). Black shale and gray siltstone facies indicate anoxic to suboxic conditions. Sequence 2 comprises the Dosagok and Gohan formations, where the Permian plant fossils (?Kazanian) occur (Chun, 1985, 1987).

A sudden fall in relative sea level formed a sequence boundary (SB 3) between the greenish gray siltstone of FA 6 and the cross-stratified pebbly conglomerate of FA 7 (Figs. 3 and 10B). The final stage of the Pyeongan depositional system (FA 7) was dominated by fluvial system, which represents lowstand systems tract of sequence 3 (Fig. 5E). FA 7 shows variable paleocurrent patterns. The high variability in paleoflows might have resulted from lateral migration of sandy braided rivers (e.g., Miall, 1977) or change in tectonic stability. FA 7 is overlain by the Cretaceous Jeokgakri Formation with angular unconformity.

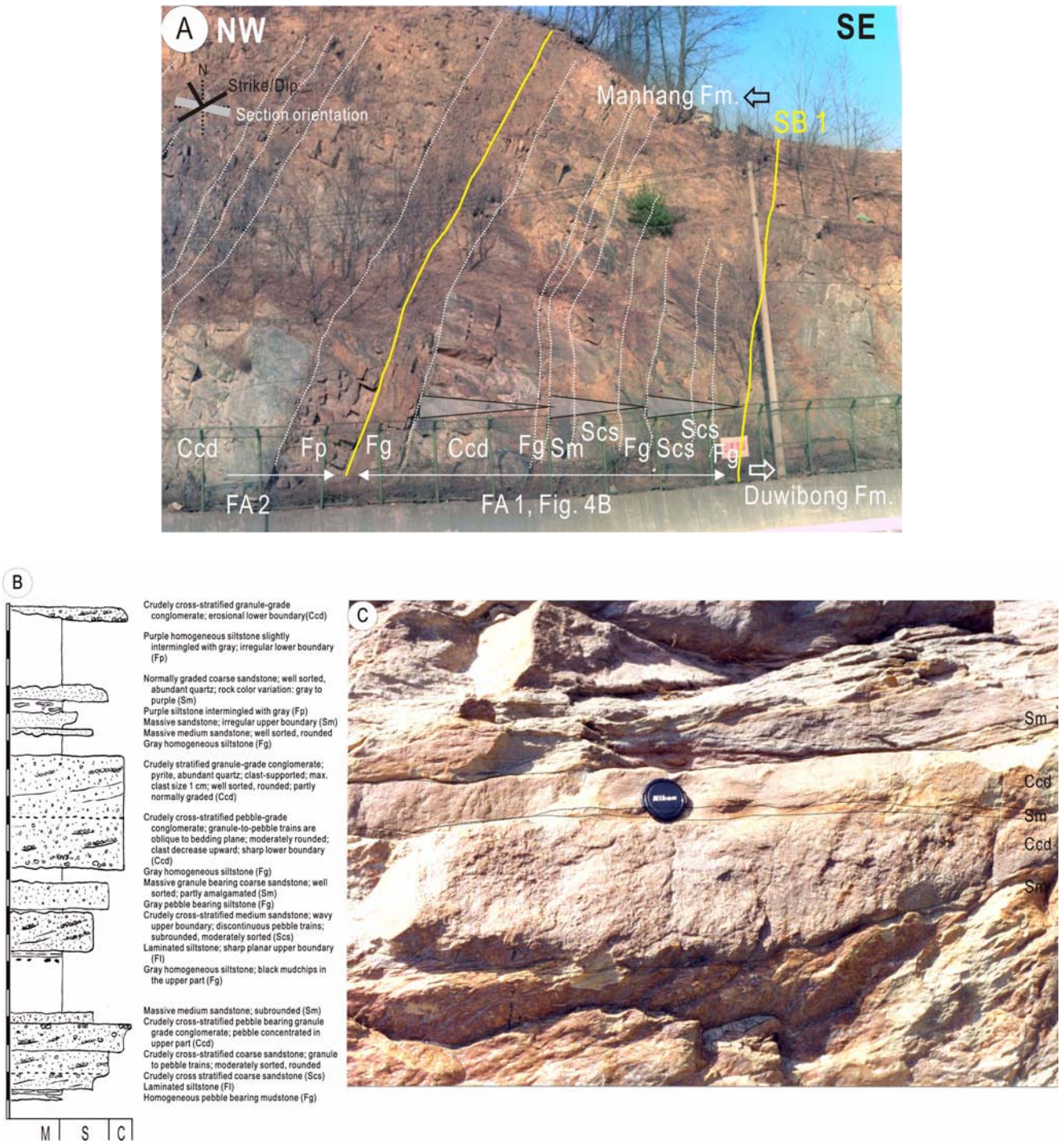

Fig. 4. A: Photograph of section 1-1 (N60°E/NW70°) represents the disconformity (SB 1) between the Manhang Formation and the underlying Joseon Supergroup. **B**: Representative detailed columnar descriptions of facies association 1, lower part of section 1-1. M = mudstone, S = sandstone, C = conglomerate. **C**: Channel- and sheet-shaped disorganized conglomerate beds are interbedded with yellowish gray fine sandstone to siltstone in facies association 2. For sedimentary facies codes, see Table 2. For section location, see Figure 1B.

5. RELATIVE SEA-LEVEL CHANGES

Figure 11 shows a relative sea-level curve in the Taebaeksan Basin, based on the changes in sedimentary facies associations and depositional systems. The changes in sea level are relative, but assumed to be small in marginal marine environments. The time interval of each depositional unit is also poorly defined due to the lack (or absence) of faunal fossils,

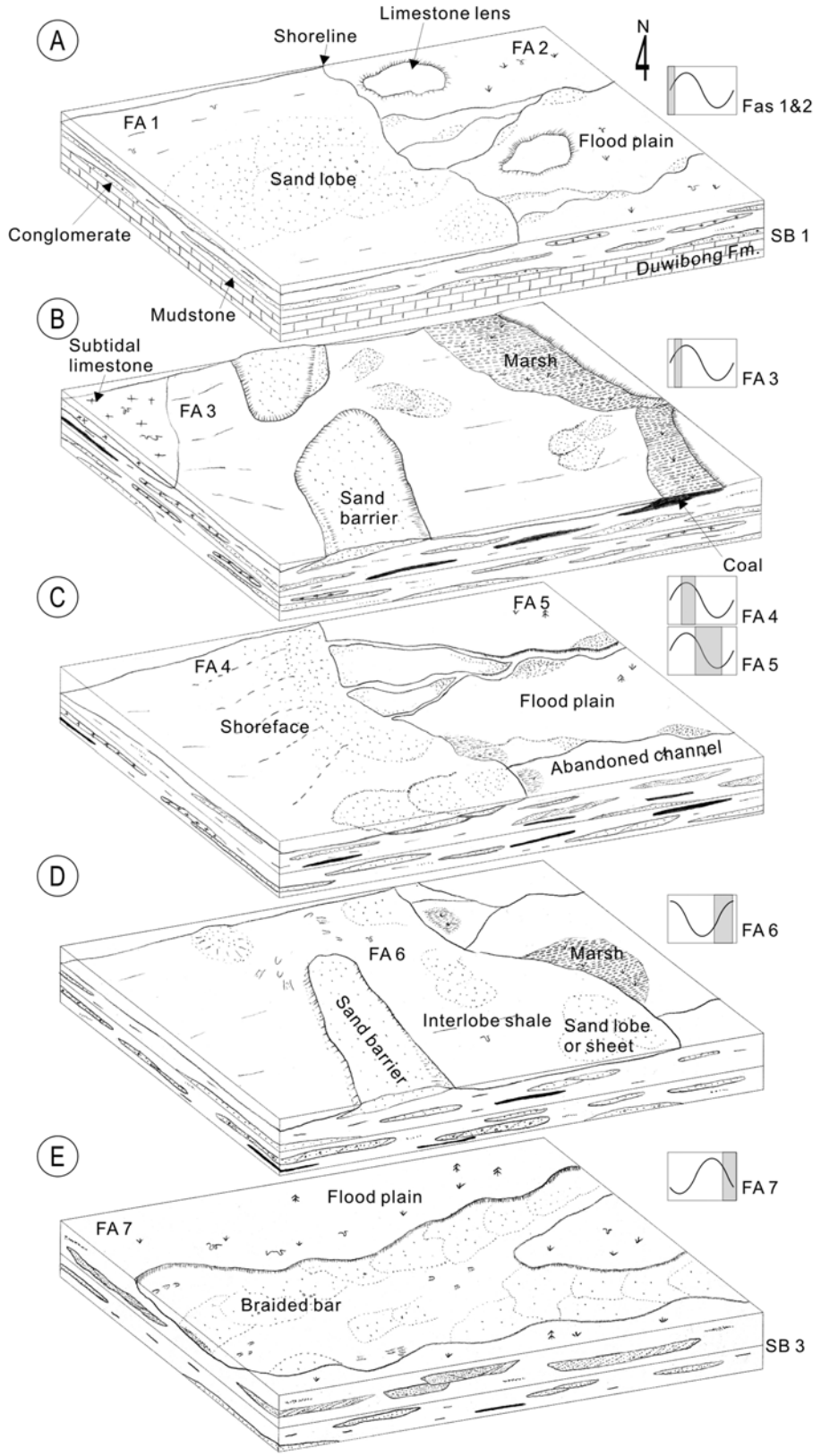

Fig. 5. Depositional model for the Hwangji Group (Pyeongan Supergroup) in the Taebaek area. **A**: Shoreface environments and coastal plain with braided rivers (Manhang Formation), **B**: Lagoonal environments (Geumcheon-Jangseong Formation), **C**: Regressive shoreface in deltaic environments (Hambaeksan Formation) and fluvial plain environments (Dosagok Formation), **D**: Restricted bay (Gohan Formation), **E**: Sandy braided river system (Donggo Formation). Shaded curve in small box represents the inferred position of relative sea level.

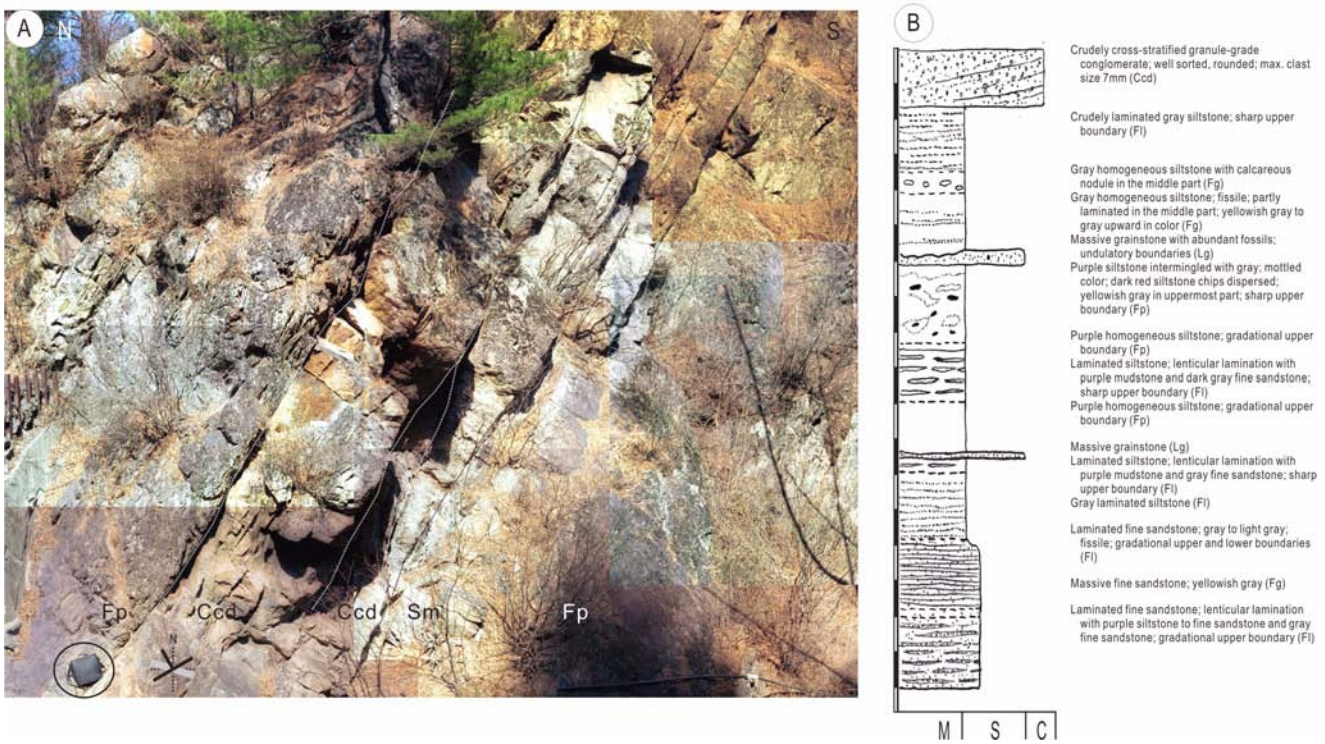

Fig. 6. A: Photograph of section 1-4 (N60°E/NW65°) shows coarse sandstone sheets and lobes with mottled purple siltstone. Bag for scale is 35 cm in width. **B**: Representative detailed columnar description of facies association 2, the upper part of section 1-5. M = mudstone, S = sandstone, C = conglomerate. For sedimentary facies codes, see Table 2. For section location, see Fig. 1B.

especially in the upper part of the sequence. Although the absolute amounts of sea-level changes are unknown, it shows three second-order cycles in the Carboniferous-Permian (Fig. 11). The first cycle most likely represents about 40 m.y. (Moscovian to Kungurian), a second-order time span (e.g., Vail et al., 1977). The second cycle most likely formed in the Guadalupian for about 14 m.y. The final regressive phase of sequence 3 probably continued for the Lopingian (Fig. 11). The sea-level curve for the Sino-Korean Block (Lin et al., 1995; Liu et al., 1997) is generally similar to that of the Taebaeksan Basin, but displays a third-order cycle within a general trend of second order cycle (Fig. 11). For the Pangea and eustasy, the trend is similar to the Taebaeksan Basin in the Carboniferous (Fig. 11). On the other hand, the curve for the South China Block is generally different from that of the Taebaeksan Basin.

The first transgression in the Taebaeksan Basin began in the Middle Carboniferous and continued to the Cisuralian (Fig. 11). The initial rise of relative sea level and the following transgression were generally synchronized with eustasy and those of the Pangea and the Hubei Basin in the middle part of the Sino-Korean Block (Fig. 11, dotted line ①). Small-scale fluctuation in TST of sequence 1 was mostly concordant with those of eustasy and the Hubei Basin (Fig. 11, dotted line ②). Relative sea level in the Hubei Basin also rose during this time, supported by alternation of shallow-marine carbonates, coastal siliciclastics and coal seams (Lin et al., 1995; Liu et al., 1997). During the Carboniferous, the North China Block was stable craton, already rifted, and drifted away from the Gondwana (Yin and Nie, 1996). It implies that the basin-fill architecture of the Pyeongan Supergroup was mainly controlled by eustasy. However, the following relative sea-level fall (Fig. 11, dotted line ③) of the early Cisuralian in the Hubei Basin did not occur in the Taebaeksan Basin. A possible explanation is local tectonic movement. During this period, the Honshu microcontinent separated from the Sino-Korean Block (Cluzel et al., 1990, 1991) and excess extensional regime possibly led to local subsidence in the Taebaeksan Basin.

Sequence 2 represents a second-order regressive-transgressive cycle that developed during the Guadalupian. In the Taebaeksan Basin, relative sea-level fall from the late Cisuralian to early Guadalupian is not in agreement with that of eustasy, implying that tectonic movements affected the change in relative sea level (Fig. 11, dotted lines ④ and ⑤). Relative sea-level fall in the Sino-Korean Block is represented by thick fluvial deposits and southward shift of the depocenter (Liu, 1990). In this period, the Sino-Korean Block sutured to the Mongolian terranes (Traynor and Sladen,

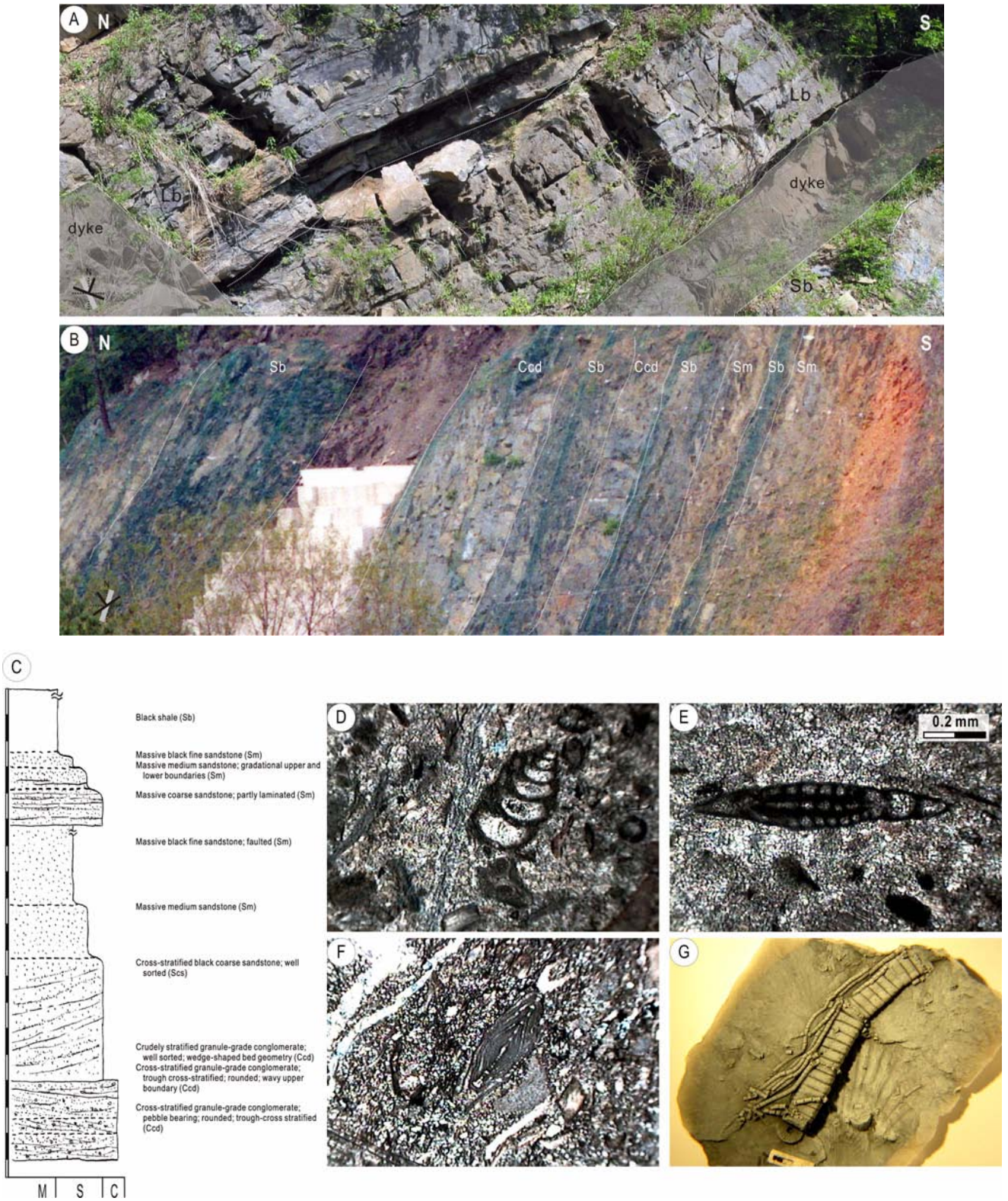

Fig. 7. A: Several meter-scale bioturbated packstone facies interlayered with chert is dominant in Section 2-a (N15°W/NE35°) of the Geumcheon-Jangseong Formation. **B**: Section 2-1 (N55°E/NW80°) is characterized by an alternation of black shale and sandstone in the lower part of the Geumcheon-Jangseong Formation. **C**: Representative detailed columnar description of facies association 3, section 2-2. M = mudstone, S = sandstone, C = conglomerate. For sedimentary facies codes, see Table 2. For section location, see Fig. 1B. **D-F**: Photomicrographs of microfossils in section 2-a, FA 3 (Geumcheon-Jangseong Fm.). **D**: foraminifera, **E**: fusulinid, **F**: nummulitid, same magnification for all photomicrographs, **G**: Crinoid stem with cirri in section 2-1, FA 3 (Geumcheon-Jangseong Fm.). Scale bar is 0.2 mm long.

Fig. 8. Photographs of the Hambaeksan Formation (FA 4). **A**: The lowermost part of the Hambaeksan Formation occurs in section 3-1 (N65°E/NW70°) and comprises thick-bedded sandstone to conglomerate intercalated with greenish gray siltstone and black shale. **B**: Westward prograding granule conglomerate occurs in section 3-4. For section location, see Figure 1B.

Fig. 9. Photograph of section 3-2 (N30°E/NW75°) shows the boundary (SB 2) between the Hambaeksan (FA 4) and Dosagok (FA 5) formations. For sedimentary facies codes, see Table 2. For section location, see Figure 1B.

Fig. 10. Photographs of Gohan and Donggo formations. **A**: Section 4-1 (EW/N80°) includes the boundary between the Dosagok (FA 5) and Gohan (FA 6) formations and comprises upward-fining units from massive sandstone to dark gray siltstone. **B**: Photograph of section 5-1 (N25°E /NW55°) shows the boundary between Dosagok (FA 6) and Donggo (FA 7) formations. Sequence boundary (SB 3) is placed at the top of the Gohan Formation. The middle part of the section is covered.

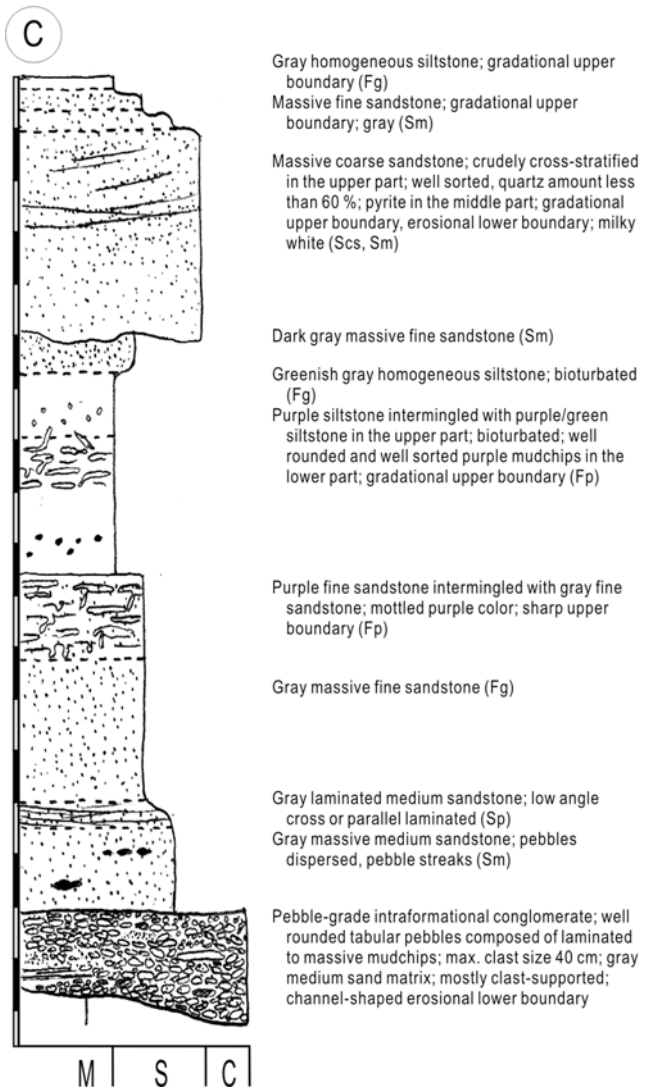

Fig. 10. (continued) **C**: Representative detailed columnar descriptions of facies associations 3, the lower part of section 5-1. M = mudstone, S = sandstone, C = conglomerate.

1995; Yin and Nie, 1996; Zorin, 1999). Rapid southward movement of the depocenter in the Sino-Korean Block resulted from collision with the Mongolian plate and formed a thick fluvial succession (400-600 m thick) in the northern margin of the block. Relative sea-level fall in the Taebaeksan basin began in the late Cisuralian. In the Hubei Basin, it occurred in the middle Cisuralian, suggesting that tectonic uplift occurred earlier in the Hubei Basin and propagated eastward. The following relative sea-level rise in the Taebaeksan Basin is not in agreement with those of the Pangea and the Hubei Basin, whereas partly similar to that of the South China Block (Fig. 11, dotted line ⑥). During this period, initial phase of the collision between the Sino-Korean and the South China blocks may have started (Ree et al., 1996; Chough et al., 2000).

Relative sea-level fall of sequence 3 in the Taebaeksan Basin occurred in the Lopingian (Fig. 11, dotted line ⑦). This fall was earlier than that of eustasy. The global sea-level fall was near its Phanerozoic minimum at the end of the Permian (Ross and Ross, 1988). Throughout the upper Permian, the collision between the Sino-Korean and South China blocks began from east to west, which continued during the Triassic (Yin and Nie, 1996). This tectonic movement influenced the changes in relative sea-level in both the South China Block and Taebaeksan Basin. The change in sediment provenance from recycling of intensely weathered granitic material to first-cycle granitic basement rocks (Lee, 1990a, 1990b, 2002; Lee and Sheen, 1998; Yu et al., 1997) and the discripance between relative sea-level curve and eustasy are indicative of tectonic movement in the Taebaeksan Basin.

The disconformity between the Joseon and the Pyeongan supergroups suggests that the Taebaeksan Basin subsided during the Cambro-Ordovician and slowly uplifted prior to marine incursion in the Middle Carboniferous. This discontinuity also occurs in the Sino-Korean Block (Hu et al., 1989; Kim et al., 2000). During the Paleozoic, the Taebaeksan Basin was part of large, slowly subsiding intracratonic sag basin of the Sino-Korean Block. The average rates of subsidence in intracratonic sag basin may have varied from less than 10 to 25 m/my, including periods of nondeposition and erosion (e.g., Einsele, 2000). The estimated subsidence rate of the Taebaeksan Basin was about 10 m/m.y. for the Paleozoic and 30 m/m.y. for the Permian. Relatively high subsidence rate for the Permian is also suggestive of tectonic subsidence, in addition to long-term thermal contraction and intraplate stress. The Taebaeksan Basin was largely controlled by eustasy in the Carboniferous, whereas tectonic movement played a role in the Permian.

6. CONCLUSIONS

1. The Pyeongan Supergroup (Hwangji Group in the Taebaek area) comprises deposits of shoreface (FA 1), coastal plain (FA 2), lagoon (FA 3), deltaic shoreface (FA 4), fluvial plain (FA 5), restricted bay (FA 6) and braided river (FA 7) environments. The changes in depositional environments were largely due to fluctuations in relative sea level.

2. The entire succession can be divided into three sequence stratigraphic units. Sequence 1 consists of initial transgressive systems tract and the subsequent highstand deposits (FAs 1, 2, 3 and 4). Sequence 2 represents lowstand fluvial system and the following transgressive bay environments (FAs 5 and 6). Sequence 3 (FA 7) consists of fluvial sequence formed during sea-level fall.

3. The relative sea-level curve for the Taebaeksan Basin

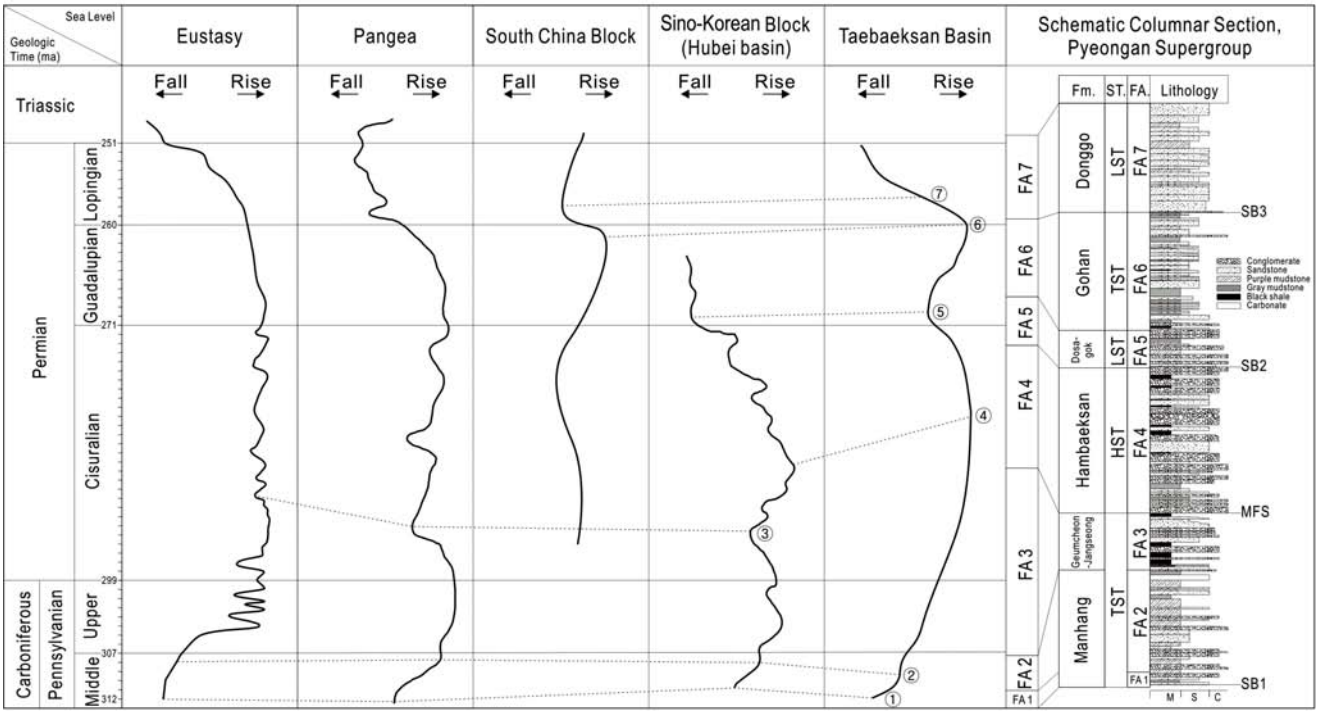

Fig. 11. The upper Paleozoic relative sea-level changes in the Taebaeksan Basin compared with those of the Pangea (Golonka and Ford, 2000), the South China Block (Chen et al., 1997), the Hubei Basin in the Sino-Korean Block (Lin et al., 1995), and eustasy (Ross and Ross, 1988). Dotted lines indicate correlation by trough to trough and peak to peak.

is generally concordant with second-order eustasy during the Carboniferous. It implies that eustasy was important for the evolution of the Taebaeksan Basin. Local tectonics played a role in the Permian.

ACKNOWLEDGMENTS: The research was supported by the Korea Science and Engineering Foundation (R14-2003-017-01000-0) and BK21 project, Ministry of Education and Human Resources. We thank D.K. Choi, D.J. Lee, Y.K. Kwon, S.M. Lee, J. Woo and Y.J. Shinn for discussion in the field. We also gratefully acknowledge helpful reviews of Dr. W.H. Ryang and an anonymous reviewer.

REFERENCES

Aigner, T., 1985, Storm Depositional Systems. Lecture Notes in Earth Sciences 3, Springer-Verlag, New York, 174p.

Allen, J.R.L., 1982, Sedimentary Structures; Their Character and Physical Basis. Elsevier, Amsterdam, 593p.

Allen, J.R.L., 1984, Parallel lamination developed from upper stage plane beds: a model based on the larger coherent structures of the turbulent boundary layer. Sedimentary Geology, 39, 227–242.

Bentham, P.A., Talling, P.J. and Burbank, D.W., 1993, Braided stream and floodplain deposition in a rapidly aggrading basin: the Escanilla Formation, Spanish Pyrenees. In: Best, J.L., Bristow, C.S. (Eds.), Braided Rivers. Geol. Soc. Lond. Spec. Publ., 75, 177–194.

Bridge, J.S., 1981, Bed shear stress over subaqueous dunes, and the transition to upper-stage plane beds. Sedimentology, 28, 33–36.

Bridge, J.S., 1993, Description and interpretation of fluvial deposits: a crtical perspective. Sedimentology, 40, 801–810.

Cabrera, L. and Saez, A., 1987, Coal deposition in carbonate-rich shallow lacustrine system: the Calaf and Mequinenza sequences (Oligocene, eastern Ebro Basin, NE Spain). J. Geol. Soc. London, 144, 451–461.

Chen, Z.Q., Yugan, J. and Shi, G.R., 1997, Permian transgression-regression sequences and sea-level changes of South China. In: Shi, G.R., Archbold, N.W., Grover, M. (Eds.), The Permian System: Stratigraphy, Paleogeography and Resources. Royal Society of Victoria, Victoria, pp. 345–368.

Cheong, C.H., 1969, Stratigraphy and paleontology of the Samcheog coalfield, Gangweondo, Korea (1). J. Geol. Soc. Korea, 5(1), 13–56.

Cheong, C.H., 1973, A Paleontology study of the fusulinids from the Samcheog coalfield, Korea. J. Geol. Soc. Korea, 9, 47–48 (in Korean with English abstract).

Chough, S.K., Kwon, S.-T., Ree, J.-H., Choi, D.K., 2000, Tectonic and sedimentary evolution of the Korean Peninsula: a review and new view. Earth-Science Reviews, 52, 175–235.

Chun, H.Y., 1985, Permo-Carboniferous plant fossils from the Samcheog Coalfield, Gangweon-do, Korea (1). Journal of the Paleontological Society of Korea 1, 95–122.

Chun, H.Y., 1987, Permo-Carboniferous plant fossils from the Samcheog Coalfield, Gangweon-do, Korea (2). Journal of the Paleontological Society of Korea 3, 1–27.

Cluzel, D., Cadet, J.P., Lapierre, H., 1990, Geodynamics of the Ogcheon belt (South Korea). Tectonophysics, 183, 41–56.

Cluzel, D., 1991, Late Palaeozoic to early Mesozoic geodynamic evolution of the Circum-Pacific orogenic belt in South Korea and Southwest Japan. Earth and Planetary Science Letters, 108, 289–305.

Collinson, J.D., Thompson, D.B., 1989, Sedimentary Structures (2nd Ed.). Unwin Hyman, London, 207p.

Davies, S.J., Gibling, M.R., 2003, Architecture of coastal alluvial deposits in an extensional basin: the Carboniferous Joggins Formation of eastern Canada. Sedimentology, 50, 415–439.

Einsele, G., 2000, Sedimentary Basins: Evolution, Facies, and Sedimentary Budget. Springer, Heidelberg, 792p.

Geological Investigation Corps of Taebaegsan Region (GICTR), 1962, Geologic Atlas of Taebaegsan Region, Geological Society of Korea.

Golonka, J., Ford, D., 2000, Pangean (Late Carboniferous-Middle Jurassic) Paleoenvironment and lithofacies. Paloegeography, Paleoclimatology, Paleoecology, 161, 1–34.

Harms, J.C., Southard, J.B., Spearing, D.R., Walker, R.G., 1982, Structures and sequences in clastic rocks, SEPM Short Course No. 9, Calgary, 161p.

Heckel, P.H., 1972, Possible inorganic origin for stromatactis in calcilutite mounds in the Tully Limestone, Devonian of New York. Journal of Sedimentary Petrology, 42, 7–18.

Hjellbakk, A., 1997, Facies and fluvial architecture of a high-energy braided river: the Upper Proterozoic Seglodden Member, Baranger Peninsula, northern Norway. Sedimentary Geology, 114, 131–161.

Hu, J., Xu., S., Tong, X., Wu., H., 1989, The Bohay Bay Basin. In: Zhu, X., (Ed.) Chinese Sedimentary Basins. Elsevier, Amsterdam, pp. 89–106.

Izart, A., Stephenson, R., Vai G. B., Vachard, D., Nindre Y.L., Vaslet, D., Fauvel P.J., Suss, P., Kossovaya, O., Chen, Z., Maslo, A., Stovba, S., 2003, Sequence stratigraphy and correlation of late Carboniferous and Permian in the CIS, Europe, Tethyan area, North Africa, Arabia, China, Gondwanaland and the USA. Paleogeography, Paleoclimatology, Paleoecology, 196, 59–84.

Jo, H.R., Chough, S.K., 2001, Architectural analysis of fluvial sequences in the northwestern part of Kyongsang Basin (Early Cretaceous), SE Korea. Sedimentary Geology, 144, 307–334.

Kawasaki, S., 1927, The flora of the Heian System, Pt. 1. Bulletin of the Geological Survey of Chosen 6, No. 1.

Korean Research Institute of Geoscience And Mineral Resources (KIGAM), 1979, Geological Atlas of the Samcheog Coalfield. 1:25,000 and Geology of the Samcheog Coalfield (Explanatory text).

Kim, H.M., 1978, Neritic paleocurrent analysis of Pennsylvanian Tethyan sea at Samcheog coalfield, Korea. Journal of Korean Institute of Mining Geology, 11, 21–38.

Kim, J.H., 1994, Structure in the Taebaeksan zone. In: Ree, J.H., Cho, M., Kwon, S.T., Kim, J.H. (Eds.), Structure and Metamorphism of the Ogcheon Belt: Field Trip guidebook. IGCP Project 321 Organizing Committee, pp. 23–57.

Kim, J.H. and Kee, W.S., 1991, Tectonic significances of the Soonchang shear zone, the Hwasum coalfield, Korea. J. Geol. Soc. Korea, 27, 642–655.

Kim, J.H. and Won, C.H., 1987, Structural analysis of Hwangji-area, Samcheog coalfield, Korea. J. Geol. Soc. Korea, 23, 136–144.

Kim, J.H., Lee, J. and Lee, H.B., 1988, Geological structures of the Baeksan-Sangcheolam area, Samcheog coalfield, Korea. J. Geol. Soc. Korea, 24, 417–430.

Kim, J.H., Lee, J.Y. and Nam, K.H., 1994, Pre-Jurassic thrust movement in Danyang area, Danyang coalfield, Korea. J. Geol. Soc. Korea, 30, 35–40 (in Korean with English abstract).

Kim, J.H., Lee, Y.I., Li, M. and Bai, Z., 2000, Comparison of the Ordovician-Carboniferous boundary between Korea and NE China: implications for correlation and tectonic evolution. Gondwana Research, 4, 39–53.

Ko, J.H., Yu, K.M., Rhee, B.K., Lee, J.Y. and Shin, J.B., 1999, Sandstone petrology of the Pyeongan Supergroup, Taebaeksan Region, Korea: implications for the Carboniferous-Triassic tectonic history of East Asia. Journal of Sedimentary Research, 69, 711–719.

Kodaira, R., 1924, Note on a new species of Schizoneura from Chosen (Korea). Japan Journal of Geology and Geography, 3, 3–4 (Japanese).

Lee, H.S., Chough, S.K., 2006, Refined lithostratigraphy and depositional environments of the Pyeongan Supergroup (Carboniferous-Permian) in the Taebaek area, mideast Korea. Journal of Asian Earth Science, 26, 339–352.

Lee, J.D., 1992, Permo-Carboniferous conodont fauna from the Samchok coal field and its biostratigraphy (I). Journal of the Paleontological Society of Korea 8, 121–131.

Lee, Y.I., 1990a, Absence of feldspar in Carboniferous Manhang (Samcheog Coalfield) and Yobong sandstones, Korea: Depositional or Diagenetic? J. Geol. Soc. Korea, 26(1), 63–69.

Lee, Y.I., 1990b, Petrofacies of the Late Carboniferous Manhang sandstones, Samcheog Coalfield and Yobong sandstones, Yeongweol coalfield. J. Geol. Soc. Korea, 26(3), 235–239.

Lee, Y.I., 2002, Provenance derived from the geochemistry of late Paleozoic-early Mesozoic mudrocks of the Pyeongan Supergroup, Korea. Sedimentary Geology, 149, 219–235.

Lee, Y.I. and Sheen, D.H., 1998, Detrital modes of the Pyeongan Supergroup (Late Carboniferous-Early Triassic) sandstones in the Samcheog coalfield, Korea: implications for provenance and tectonic setting. Sedimentary Geology, 119, 219–238.

Lin, C., Li, S., Li, Z., 1995, Facies architecture, stratigraphic sequences and coal occurrences in the Late Carboniferous and Early Permian delta complexes of the North Hubei Basin, China. In: Oti, M.N., Postam, G. (Eds.), Geology of Deltas, A.A. Balkema, Rotterdam, pp. 125–138.

Liu, G., 1990, Permo-Carboniferous paleogeography and coal accumulation and their tectonic control in the North and South China continental plates. In: Lyons, P.C., Callcot, T.G., Alpern, B. (Eds.), Peat and Coal: Origin, Facies, and Coalification. International Journal of Coal Geology, 16, 73–117.

Liu, G., Ricken, W., Mosbrugger, V., Kullmann, J., 1997, Permo-Carboniferous carbonate-coal sequences and their stacking patterns in the North China Block. In: Shi, G.R., Archbold, N.W., Grover, M. (Eds.), The Permian System: Stratigraphy, Paleogeography and Resources. Royal Society of Victoria, Victoria, pp. 369–384.

McCabe, P.J., 1984, Depositional environments of coal and coal bearing strata. In: Rahmani, R.A., Flores, R.M. (Eds.), Sedimentology of Coal and Coal bearing Sequences, International Association of Sedimentologists Special Publication 7, Blackwell, London, pp. 13–42.

Miall, A.D., 1977, A review of the braided-river depositional environment. Earth-Science Reviews, 13, 1–62.

Miall, A.D., 1978, Lithofacies types and vertical profile models in braided river deposits: a summary. In: Miall, A.D., (Ed.), Fluvial Sedimentology. Canadian Soc. Petroleum Geologists Memoir 5, pp. 596–604.

Miall, A.D., 1985, Architectural-element analysis: a new method of facies analysis applied to fluvial deposits. Earth-Science Reviews, 22, 261–308.

Miall, A.D., 1996, The Geology of Fluvial Deposits. Springer, Berlin, 582p.

Nemec, W. and Postma, G., 1993, Quaternary alluvial fans in southwestern Crete: Sedimentation processes and geomorphic evolution. In: Marzo, M., Puigdefabregas, C. (Eds.), Alluvial Sedimentation. Int. Assoc. Sediment. Spec. Publ., 17, pp. 235–276.

Plint, A.G., Wadsworth, J.A., 2003, Sedimentology and paleomorphology of four valley systems incising delta plains, western Canada Foreland Basin: implication for mid-Cretaceous sea-level changes. Sedimentology, 50, 1147–1189.

Posamentier, H.W. and Vail, P.R., 1988, Eustatic controls on clastic deposition I – sequence and systems tract model. In: Wilgus, C.K., Hastings, B.S, Kendall, C.G.St.C., Posamentier, H.W., Ross, C.A., Van Wagoner, J.C. (Eds.), Sea-level changes: an integrated approach. Society of Economic Paleontologists and Mineralogists Special Publication No. 42, Oklahoma, pp. 109–124.

Reading H.G. and Collinson, J.D., 1996, Clastic coasts. In: Reading, H.G., (Ed.), Sedimentary Environments: Processes, Facies and Stratigraphy. Blackwell, London, pp. 154–231.

Ree, J.H, Cho, M., Kwon, S.T. and Nakamura, E., 1996, Possible eastward extension of Chinese collision belt in South Korea: the Imjingang belt. Geology, 24, 1071–1074.

Rhoads, D.C., 1967, Biogenic reworking of intertidal and subtidal sediments in Barnstable Harbor and Buzzards Bay, Massachusetts. Journal of Geology, 75, 461–476.

Ross, C.A. and Ross, J.R.P., 1985, Late Paleozoic depositional sequences are synchronous and worldwide. Geology, 13, 194–197.

Ross, C.A. and Ross, J.R.P., 1988, Late Paleozoic transgressive-regressive deposition. In: Wilgus, C.K., Hastings, B.S, Kendall, C.G.St.C., Posamentier, H.W., Ross, C.A., Van Wagoner, J.C. (Eds.), Sea-level changes: an integrated approach. Society of Economic Paleontologists and Mineralogists Special Publication No. 42, Oklahoma, pp. 227–247.

Ryu, I.C., Doh, S.J., Paik, K.H. and Choi, S.G., 1997, Stratigraphic reconsideration of the Permian Jangseong Formation, Samcheog coalfield, Journal of the Geological Society of Korea, 33, 78–86 (in Korean with English abstract).

Scotese, C.R., Boucot, A.J. and McKerrow, W.S., 1999, Gondwanan palaeogeography and palaeoclimatology. Journal of African Earth Sciences, 28, 99–114.

Shiraki, T., 1930, Geological map of the Samch'ok coalfield.

Shiraki, T., 1940, The Samcheok Coalfield in the Kangweon-do, Korea. Report on Coalfield survey, Korea, 14p.

Simpson, E.L, Dilliard, K.A., Rowell, B.F. and Higgins, D., 2002, The fluvial-to-marine transition within the post-rift Lower Cambrian Hardyston Formation, Eastern Pennsylvania, USA. Sedimentary Geology, 147, 127–141.

Tateiwa, I., 1931, Occurrence of ore deposit and stratigraphy of the Proterozoic Era to Jurassic Period in Sungcheon region, Pyangannam-do. Journal of the Mining of Chosen.

Traynor, J.J. and Sladen, C., 1995, Tectonic and stratigraphic evolution of the Mongolian People's Republic and its influence on hydrocarbon geology and potential. Marine and Petroleum Geology, 12, 35–52.

Todd, S.P., 1989, Stream-driven, high-density gravelly traction carpets: possible deposits in the Trabeg Conglomerate Formation, SW Ireland and some theoretical considerations of their origin. Sedimentology, 36, 513–530.

Todd, S.P. and Went, D.J., 1991, Lateral migration of sand-bed rivers: examples from the Devonian Glashabeg Formation, SW Ireland and the Cambrian Alderney Sandstone Formation, Channel Islands. Sedimentology, 38(6), 997–1020.

Turner, P., 1980, Continental Red Beds. Elsevier, Amsterdam, 562p.

Vail, P.R., Mitchum, R.M. Jr. and Thompson, S.I., 1977, Global cycles of relative changes of sea level. American Association of Petroleum Geologists, Tulsa, Okla., pp. 83–97.

Van Wagoner, J.C., Posamentier, H.W., Mitchum, R.M. Jr., Vail, P.R., Sarg, J.F., Loutit, T.S. and Hardenbol, J., 1988, An overview of the fundamentals of sequence stratigraphy and key definition. In: Wilgus, C.K., Hastings, B.S, Kendall, C.G.St.C., Posamentier, H.W., Ross, C.A., Van Wagoner, J.C. (Eds.), Sea-level changes: an integrated approach. Society of Economic Paleontologists and Mineralogists Special Publication No. 42, Oklahoma, pp. 39–45.

Veevers, J.J., 2004, Gondwanaland from 605-500 Ma assembly through 320 Ma merger in Pangea to 185-100 Ma breakup: supercontinental tectonics via stratigraphy and radiometric dating. Earth-Science Reviews, 68, 1–132.

Walker, T.R., 1967, Formation of red beds in modern and ancient deserts. Geological Society of America Bulletin, 78, 353–368.

Yin, A., Nie, S., 1996, A Phanerozoic palinspastic reconstruction of China and its neighboring regions. In: Yin, A., Harrison, M. (Eds.), The tectonic evolution of asia. Cambridge University Press, New York, pp. 442–485.

Yu, K.M., Lee, G.H. and Boggs, S., 1997, Petrology of Late Paleozoic Early Mesozoic Pyeongan Group sandstones, Kohan area, South Korea and its Provenance and tectonic implications. Sedimentary Geology, 109(3-4), 321–338.

Zorin, Y.A., 1999, Geodynamics of the western part of the Mongolia-Okhotsk collisional belt, Tran-Baikal region (Russia) and Mongolia. Tectonophysics, 306, 33–56.

Manuscript received March 6, 2006
Manuscript accepted August 18, 2006